

Saturation and Scaling of Epitaxial Island Densities

C. Ratsch and A. Zangwill

School of Physics, Georgia Institute of Technology, Atlanta, Georgia 30332

P. Šmilauer* and D. D. Vvedensky

The Blackett Laboratory, Imperial College, London SW7 2BZ, United Kingdom

(Received 4 October 1993)

The aggregation of adatoms into 2D islands is studied as a function of coverage Θ and the ratio of surface diffusion rate to deposition rate $\mathfrak{N} = D/F$ by Monte Carlo simulations of a model of epitaxial growth that permits atoms to detach from island edges at a rate determined by a pair bond energy E_N . The total island density is observed to saturate before coalescence becomes important. In this regime, the density of adatoms $N_1 \sim \Theta^{-r} \mathfrak{N}^{-\omega}$ while the density of islands composed of $s > 1$ atoms $N_s \sim \Theta \langle s \rangle^{-2} g(s/\langle s \rangle)$ where the average island size $\langle s \rangle \sim \Theta \mathfrak{N}^\chi$. The exponents r , ω , and χ vary smoothly with E_N .

PACS numbers: 68.55.-a, 82.20.Mj, 61.43.Hv

Recent observations of the self-organized growth of uniformly sized and spaced quantum dots on GaAs(100) represent an important milestone in the quest to establish the principles of epitaxial architecture [1]. These experiments evolved from a long tradition of electron microscopy observations of the density of three-dimensional islands that nucleate on a surface during growth for the purpose of deducing fundamental material parameters from homogeneous rate equation treatments of the growth process [2,3]. The extension of this general approach to the case of two-dimensional (2D) islands by the use of scanning tunneling microscopy (STM) [4,5] and surface sensitive diffraction [6-8] has, in turn, sparked a renewal of interest in the corresponding theory [9].

Of particular note is the work of Bartelt and Evans [10] who performed extensive Monte Carlo simulations of *irreversible* aggregation via surface diffusion, i.e., deposited atoms that encounter and adhere to an existing island are forbidden to detach and rejoin the monomer population. It was found that the areal density of adatoms and 2D islands composed of $s \geq 1$ atoms N_s takes the form

$$N_s \sim \frac{\Theta}{\langle s \rangle^2} g(s/\langle s \rangle), \quad (1)$$

where $g(x)$ is a scaling function and $\langle s \rangle \sim \Theta^z \mathfrak{N}^\chi$ describes the dependence of the average island size on the coverage Θ and the ratio of the adatom surface diffusion rate to the deposition rate $\mathfrak{N} = D/F$. By now, confirmation of this form or its consequences has been obtained from a number of different models of irreversible aggregation [11-15] and from an STM study of Fe(100) homoepitaxy [5].

The purpose of the present Letter is to examine the question of island size scaling with an epitaxial growth model where the passage from irreversible to *reversible* aggregation can be achieved by tuning a single pair bond energy parameter. We find that adatom detachment hastens the appearance of a *precoalescence* saturation regime where the scaling form (1) always obtains for $s > 1$ while the adatom density obeys

$$N_1 \sim \Theta^{-r} \mathfrak{N}^{-\omega}. \quad (2)$$

The exponent $z = 1$ always in this regime while χ , r , and ω are found to vary smoothly as the rate at which atoms can detach from island edges increases from zero. In contrast to a simple rate theory widely used to extract microscopic parameters from growth experiments, a consistent description of our results is possible only if the rate constant for adatom attachment to islands depends on both island size and the total density of islands.

We employ a solid-on-solid model of epitaxial growth [16] that has been shown to yield surface morphologies in quantitative agreement with *in situ* surface diffraction experiments [17]. The substrate is assumed to have a simple cubic structure with unit lattice constant. Neither vacancies nor overhangs are permitted. Growth is initiated by the random deposition of atoms onto the substrate at a rate F per site. Desorption is forbidden so that $\Theta = Ft$. The rate at which *any* surface atom hops to a nearest neighbor site is determined by the configuration-dependent Arrhenius-type expression $k(T) = D \exp(-nE_N/k_B T)$ where $D = (2k_B T/h) \exp(-E_S/k_B T)$ is the free atom migration rate, $n = 0, 1, 2, 3, 4$ is the number of lateral nearest neighbors before the hop occurs, and E_N is a pair bond energy. Temperature, flux, and E_N are regarded as variable but we have set $E_S = 1.3$ eV. The number density of atoms present in the second layer above the substrate is negligible ($\ll 1\%$) despite the fact that island atoms have a nonzero probability to hop up into the second layer and deposition onto a previously nucleated island occurs frequently at the higher coverages. All results reported below represent averages over at least 25 simulations on a lattice of size 400×400 .

Figure 1 illustrates typical surface morphologies at 20% coverage for $T = 800$ K and E_N equal to 1.0 and 0.3 eV. The results bear a striking resemblance to STM images obtained by Behm and co-workers for Au/Ru(0001) [18] and Ni/Ni(001) [19], respectively. The passage from a fractal island morphology to a compact island morphology arises naturally as E_N decreases in this model because atoms with a single lateral neighbor can more

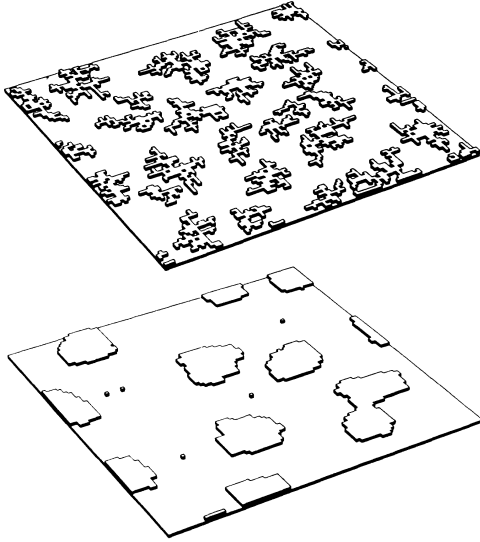


FIG. 1. Typical island morphologies at 20% coverage for a 100×100 section of a 400×400 lattice obtained by Monte Carlo simulation with $E_N = 1.0$ eV (upper panel) and $E_N = 0.3$ eV (lower panel).

readily hop away until an environment of higher coordination is found. Note, however, that islands formed by irreversible aggregation can be more compact [5,13,15] if the barrier to adatom diffusion along an island edge is less than the barrier to atom detachment from an island. These barriers are identical in the simple model discussed in this paper. Nonetheless, the fact that adatom attachment to islands is *reversible* distinguishes our work from all previous simulation studies [10–15] addressed to the question of submonolayer scaling.

Figure 2 illustrates the scaling of our simulation data for N_s when plotted as suggested by (1) at six coverages for two extreme values of the pair bond energy. The change in the scaling function that occurs when we pass from irreversible aggregation ($E_N = 1.0$ eV) to reversible aggregation ($E_N = 0.3$ eV) agrees nearly quantitatively with a corresponding scaling function change observed by Strosio and Pierce [5] for low and high temperature N_s data obtained at fixed coverage but variable \mathfrak{N} for Fe/Fe(001). The scaling with \mathfrak{N} is found by us as well since Fig. 2(a) includes simulation results obtained at two different values of \mathfrak{N} . Indeed, for $\mathfrak{N} > 10^5$ and $7.5\% \leq \Theta \leq 25\%$, our data are consistent with $\langle s \rangle \sim \Theta^z \mathfrak{N}^\chi$ with $z = 1$ and $\chi \approx 1/3$ for $E_N = 1.0$ eV and $\chi \approx 1/2$ for $E_N = 0.3$ eV. Note that the data for islands of very small size do not collapse onto the scaling curve in the latter case.

The fact that data collapse occurs for $z = 1$ is in agreement with experimental data for Pb islands on Cu(001) [8] but is not consistent with the predictions of either the point island model ($z = 2/3$) of Ref. [10] or the continuous nucleation model ($z \approx 0.34$) of Ref. [12]. To understand this behavior, we appeal to the following well-

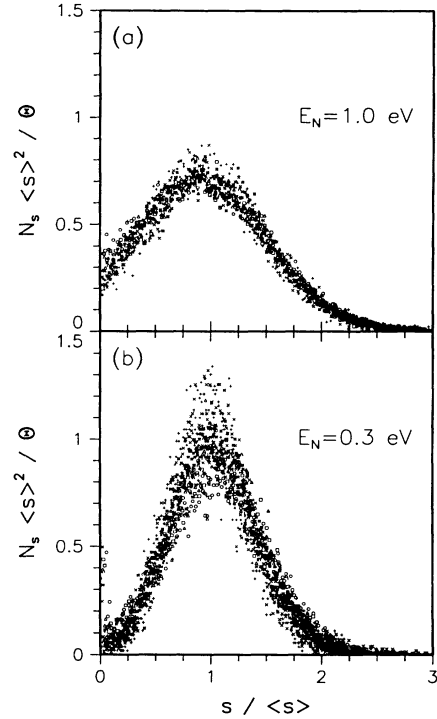


FIG. 2. Data collapse of the island size distribution function at two values of E_N for six coverages from 7.5% to 25%: (a) $E_N = 1.0$ eV [data shown for $F = 0.1$ s $^{-1}$ at $T = 750$ K ($\mathfrak{N} = 6 \times 10^5$) and $T = 800$ K ($\mathfrak{N} = 2 \times 10^6$)]; (b) $E_N = 0.3$ eV (data shown for $F = 0.1$ s $^{-1}$ at $T = 750$ K).

known [2,3,9] homogeneous rate equation description of the island growth process:

$$\begin{aligned} \frac{dN_1}{dt} &= F - K_1 N_1^2 - N_1 \sum_{s \geq 1} K_s N_s + \gamma_2 N_2 + \sum_{s > 1} \gamma_s N_s, \\ \frac{dN_s}{dt} &= N_1 (K_{s-1} N_{s-1} - K_s N_s) - \gamma_s N_s \\ &\quad + \gamma_{s+1} N_{s+1} \quad (s > 1). \end{aligned} \quad (3)$$

These mean-field equations presume that only single atoms are mobile and that islands grow and dissociate by the attachment and detachment of single atoms. Monomers attach to islands of size s at a rate K_s and detach from islands of size s at a rate γ_s . Analyses of these equations commonly define a “critical nucleus size” i such that $\gamma_s = 0$ when $s > i$. Moreover, recent analytic work [20] has focused on the choice $K_s = D\sigma_s \propto Ds^p$ where the parameter p is chosen to reflect a presumed island size dependence of the adatom capture rate. It is then easy to show [20] that (3) is solved by (1) and (2) at fixed \mathfrak{N} with $z = (i+1)r = (i+1)[i+2-p(i+1)]^{-1}$ when $0 \leq p \leq 1/(i+1)$ and $z = 1$ with $r = p$ when $1/(i+1) \leq p \leq 1$. The results of Ref. [10] correspond to $i = 1$ and $p = 0$ while our simulations are consistent with the $r = p$ regime. Thus, from (2), p can be extracted from the time evolution of the monomer density.

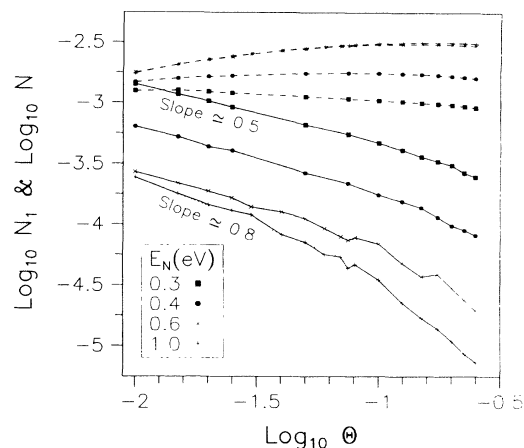


FIG. 3. Dependence of the monomer density (solid curves) and total island density (dashed curves) on coverage Θ for several values of E_N at $T=800$ K and $F=0.1$ s $^{-1}$.

The solid curves in Fig. 3 illustrate $N_1(\Theta)$ at $F=0.1$ s $^{-1}$ and $T=800$ K ($\mathfrak{N}=2 \times 10^6$) for several values of E_N . Note that the curvature of $N_1(\Theta)$ increases progressively as E_N increases. We have discovered that this phenomenon can be reproduced from the rate equations (3) only if one includes "direct hit" terms [2] that account for deposited atoms that land either (i) on top of or (ii) immediately adjacent to existing islands. Numerical integration of the rate equations with and without these terms shows that the slope of the solid curves in Fig. 3 at the *earliest* times shown are most representative of the correct values of p . We thus extract $p \approx 0.5$ for $E_N=0.3$ eV (compact islands) and $p \approx 0.8$ for $E_N=1.0$ eV (fractal islands). These numbers are readily explicable if we regard the s dependence of K_s as a measure of the number of perimeter sites. In that case, $p = d_p/d_f$ where d_p is the fractal dimension of the island perimeter and d_f is the fractal dimension of the island itself [21]. Direct measurement from images like Fig. 1 yields $d_p = 1.35 \pm 0.05$ and $d_f = 1.72 \pm 0.05$ in the fractal case. Of course, $d_f = 2d_p = 2$ for the compact case.

From (1), the integrated island density $N = \sum_{s>1} N_s \sim \Theta / \langle s \rangle \sim \Theta^{1-z} \mathfrak{N}^{-z}$ so we expect $N(\Theta) \sim \text{const}$ (or nearly so [20]) when $z=1$. Thus, in contrast to previous analytic work [2,3,9], we find that existing islands merely grow in size [22] for a finite coverage interval that begins *after* new island nucleation has been arrested by the efficient capture of adatoms by spatially extended islands but *before* island coalescence becomes significant [13]. Close inspection of the dashed curves in Fig. 3 demonstrates the veracity of this assertion most clearly for $E_N=0.3$ eV where saturation sets in at $\Theta_S \approx 2\%$. But it appears to be true as well for the fractal island case where $\Theta_S \approx 10\%$ [15]. To understand the behavior of $\Theta_S(E_N)$, we appeal to self-consistent diffusion-reaction (DR) calculations due to Venables [23] that show that the number density of adatoms is relatively depleted in a

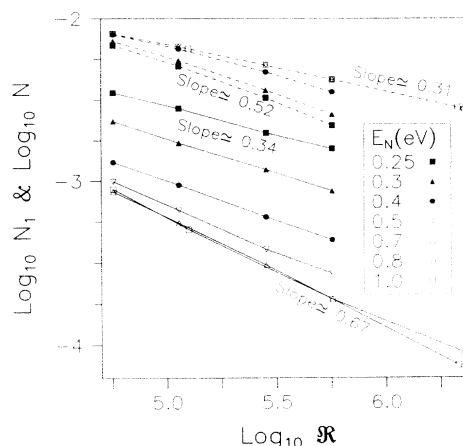


FIG. 4. Dependence of the monomer density (solid curves) and total island density (dashed curves) on $\mathfrak{N}=D/F$ for several values of E_N at 5% coverage.

zone that extends a distance $\lambda \approx 1/\sqrt{\langle \sigma \rangle N}$ away from each island edge. The quantity $\langle \sigma \rangle$ [the average value of the capture coefficient σ_s defined below (3)] is proportional to the gradient of the adatom concentration evaluated at the island edge. But compared to the perfect-sink results presented in Ref. [23], related DR calculations [24,25] suggest that the latter quantity will be *reduced* if kinetic processes such as adatom detachment are present at the island edge. The trend observed above thus can be rationalized since the nucleation of new islands is effectively suppressed throughout the depletion zone.

We turn finally to the \mathfrak{N} dependence of N and N_1 . As shown in Fig. 4, the simulations do indeed yield the power law behavior $N_1 \sim \mathfrak{N}^{-\omega}$ and $N \sim \mathfrak{N}^{-\chi}$ noted earlier for all values of E_N . But a straightforward extension of the analysis of Ref. [20] to the case of variable \mathfrak{N} yields scaling relations between the exponents χ and ω that are not satisfied by our data. We obtain a consistent description within the homogeneous rate equation formalism only if the rate at which adatoms are captured by islands is presumed to take the form $K_s \propto DN^q s^p$ (and $K_1 \propto D$). The predictions that $z=1$ and $r=p$ when $1/(i+1) \leq p < 1$ survive this change and we find in addition that

$$\omega = \frac{2+q-p}{i(1+q-p)+2+q-p}, \quad (4)$$

$$\chi = \frac{i}{i(1+q-p)+2+q-p}.$$

Operationally, we use the measured values of χ , ω , and p at $\Theta=5\%$ to extract values of q and i . The results are summarized in Table I except for the interval $0.45 < E_N < 0.75$ where p and ω vary with \mathfrak{N} (cf. Fig. 4). As expected, we find a critical nucleus size $i=1$ for the fractal islands and values for ω and χ that agree with the results of other studies for the case of irreversible island formation [10,14,15]. The general trend that i increases

TABLE I. Scaling exponents and the parameter i as a function of E_N .

E_N (eV)	p	ω	χ	q	i
0.25	0.50(5)	0.34(3)	0.52(2)	0.8(2)	3.5(3)
0.3	0.50(5)	0.43(3)	0.47(2)	0.7(2)	2.4(3)
0.4	0.50(5)	0.48(3)	0.40(2)	0.8(2)	2.4(2)
0.8	0.80(5)	0.67(2)	0.33(3)	0.8(2)	1.0(1)
1.0	0.80(5)	0.67(2)	0.33(3)	0.8(2)	1.0(1)

as the pair bond energy decreases is consistent with qualitative expectations although small corrections to (4) may be required in the postsaturation regime. We note also that $i > 1$ tends to enhance the suppression of nucleation within the depletion zones [23]. In any event, the noninteger values obtained for i make clear that this quantity is best interpreted as an *effective* critical nucleus size that permits the mean field equations (3) and (4) to mimic the behavior of simulations (and experiment).

Our claim that explicit s and N dependence must be retained in the adatom capture rate K_s appears to contradict repeated statements in the literature that $\langle K \rangle = D \langle \sigma \rangle$ is sufficient with a *constant* value for the "capture number" $\langle \sigma \rangle$ [2,3]. But, in fact, the DR calculations noted above [23] demonstrate that $\langle \sigma \rangle$ is a smooth function of the product $\langle s \rangle N$ that can be fitted to a power law over any limited interval of coverage. In the regime of coverages studied here, these calculations yield $0.5 < p = q < 0.8$ in our notation (cf. Table I). So in what sense is $\langle \sigma \rangle$ constant? Since $\langle s \rangle \sim \Theta^z \eta^{\chi}$, it is the case that $\langle \sigma \rangle \sim \Theta^{z(p-q)+q} \eta^{\chi(p-q)}$. As noted, $p = q$ in the DR calculations and $\chi |p - q| \ll 1$ using the values reported in Table I for any E_N . Thus, if one focuses only on the single exponent χ , simulations and experiments will appear to be interpretable using a rate equation theory that assumes $p = q = 0$. But, for example, the scaling relation $\omega + \chi = 1$ [10] (that obtains when $p = q$) is violated when adatom detachment from islands becomes significant.

We thank Steve Bales, Fereydoon Family, John Venables, and Dietrich Wolf for useful discussions. We are particularly indebted to Jim Evans for pointing out to us the full consequences of the scaling form (1). Work at Georgia Tech was performed with support from the U.S. Department of Energy under Grant No. DE-FG05-88ER45369. Work at Imperial College was performed with support from a NATO travel grant and the Research Development Corporation of Japan.

*Also at Interdisciplinary Research Centre for Semiconductor Materials, Imperial College, London SW7 2BZ, United Kingdom; on leave from the Institute of Physics, Czech Academy of Science, Cukrovarnická 10, 16200

Praha 6, Czech Republic.

- [1] D. Leonard, M. Krishnamurthy, C. M. Reeves, S. P. Denbairs, and P. M. Petroff, *Appl. Phys. Lett.* **63**, 23 (1993); J. M. Moison, F. Houzay, F. Barthe, L. Leprince, E. André, and O. Vatel, *ibid.* **64**, 196 (1994).
- [2] J. A. Venables, G. D. T. Spiller, and M. Hanbücken, *Rep. Prog. Phys.* **47**, 399 (1984).
- [3] S. Stoyanov and D. Kashchiev, in *Current Topics in Materials Science*, edited by E. Kaldis (North-Holland, Amsterdam, 1981), Vol. 7, pp. 69–141.
- [4] Y. W. Mo, J. Kleiner, M. B. Webb, and M. Lagally, *Phys. Rev. Lett.* **66**, 1998 (1991).
- [5] J. A. Stroschio and D. T. Pierce, *Phys. Rev. B* **49**, 8522 (1994).
- [6] J.-K. Zuo and J. F. Wendelken, *Phys. Rev. Lett.* **66**, 2227 (1991).
- [7] H.-J. Ernst, F. Fabre, and J. Lapujoulade, *Phys. Rev. B* **46**, 1929 (1992).
- [8] W. Li and G. Vidali, *Phys. Rev. B* **48**, 8336 (1993).
- [9] J. Villain, A. Pimpinelli, L.-H. Tang, and D. Wolf, *J. Phys. I (France)* **2**, 2107 (1992); J. Villain, A. Pimpinelli, and D. Wolf, *Comments Condens. Matter Phys.* **16**, 1 (1992).
- [10] M. Bartelt and J. W. Evans, *Phys. Rev. B* **46**, 12675 (1992); *Surf. Sci.* **298**, 421 (1993).
- [11] L.-H. Tang, *J. Phys. (France)* **I 3**, 935 (1993).
- [12] T. Nagatani, *J. Phys. Soc. Jpn.* **62**, 981 (1993).
- [13] G. T. Barkema, O. Biham, M. Brennan, D. O. Boerma, and G. Vidali, *Surf. Sci. Lett.* **306**, L569 (1994). Adatom detachment from island edges technically is not forbidden in the model used here. But the authors remark that essentially no detachment actually occurs at the temperatures used in the simulations.
- [14] J. G. Amar, F. Family, and P.-M. Lam (unpublished).
- [15] G. S. Bales and D. C. Chrzan (unpublished); G. S. Bales (private communication).
- [16] S. Clarke and D. D. Vvedensky, *J. Appl. Phys.* **63**, 2272 (1988).
- [17] T. Shitara, D. D. Vvedensky, M. R. Wilby, J. Zhang, J. H. Neave, and B. A. Joyce, *Phys. Rev. B* **46**, 6815 (1992); **46**, 6825 (1992).
- [18] R. Q. Hwang, J. Schroder, C. Gunther, and R. J. Behm, *Phys. Rev. Lett.* **67**, 3279 (1991).
- [19] E. Kopatzki, S. Gunther, W. Nichtl-Pecher, and R. J. Behm, *Surf. Sci.* **284**, 154 (1993).
- [20] J. A. Blackman and A. Wilding, *Europhys. Lett.* **16**, 115 (1991); N. V. Brilliantov and P. L. Krapivsky, *J. Phys. A* **24**, 4787 (1991).
- [21] R. F. Voss, in *Scaling Phenomena in Disordered Systems*, edited by R. Pynn and A. Skjeltorp (Plenum, New York, 1985), p. 1.
- [22] When the pair bond energy is small, dimers dissociate so that the total number density of islands with $s > 1$ actually decreases slightly within the "saturation" regime.
- [23] J. A. Venables, *Philos. Mag.* **27**, 697 (1973). See especially sections 4 and 5 and Figures 2 and 4.
- [24] A. A. Chernov, *Modern Crystallography III* (Springer-Verlag, Berlin, 1984), Sec. 3.2.1.
- [25] R. Ghez and S. S. Iyer, *IBM J. Res. Dev.* **32**, 804 (1988).